Numerical analysis of a new mixed-formulation for eigenvalue convection-diffusion problems

Charles Pierre, Franck Plouraboué

Numerical analysis of a new mixed-formulation for eigenvalue convection-diffusion problems

C. Pierre   F. Plouraboué

Abstract

A mixed formulation is proposed and analyzed mathematically for coupled convection-diffusion in heterogeneous medias. Transfer in solid parts driven by pure diffusion is coupled with convection/diffusion transfer in fluid parts. This study is carried out for translationnaly invariant geometries (general infinite cylinders) and unidirectional flows. This formulation brings to the fore a new convection/diffusion operator, the properties of which are mathematically studied : its symmetry is first shown using a suitable scalar product. It is proved to be self-adjoint with compact resolvent on a simple Hilbert space. Its spectrum is characterized as being composed of a double set of eigenvalues: one converging towards $-\infty$ and the other towards $+\infty$, thus resulting in a non-sectorial operator. The decomposition of the convection-diffusion problem into a generalized eigenvalue problem permits the reduction of the original three-dimensional problem into a two-dimensional one. Despite being non sectorial, a complete solution on the infinite cylinder, associated to a step change of the wall temperature at the origin, is exhibited with the help of the operator's two sets of eigenvalues/eigenfunctions. On the computational point of view, a mixed variational formulation is naturally associated to the eigenvalue problem. Numerical illustrations are provided for axi-symmetrical situations, the convergence of which is found to be consistent with the numerical discretization.

Keywords Convection-diffusion · variational formulation · Hilbert space · mixed formulation

1 Introduction

Convection-diffusion problems are of importance in many fields of applications in thermal, chemical or biomedical engineering sciences. More specifically, heat or mass diffusion coupled with unidirectional convection is present in many types of equipments such as heat pipes, heat exchangers (shell, tube or plate), chromatographs and reactors and mass exchangers in micro-channel articial devices, and occurs in real biological tissues. This framework covers both parallel or counter flow configurations. A classical strategy for describing the temperature field T of tube like configurations in the applied literature is generally to assume the following separate-variable

decomposition:

$$T(x, y, z) = \sum_{\lambda \in \Lambda} c_\lambda T_\lambda(x, y) e^{\lambda z}, \tag{1}$$

where z is the longitudinal coordinate along which the flow is aligned and x, y are transverse coordinates. The usual subsequent steps [7] are then to search for the "*eigenvalues/eigenfunctions*" λ/T_λ and finally compute the amplitude coefficients c_λ.

This strategy, although well established, raises several important questions. To our knowledge, there is no complete theoretical foundation for decomposition (1). This lack of theoretical framework, despite commonly used terminology, does not permit Λ and T_λ to be defined via an eigenvalue problem, all the more so a symmetrical one. On the one hand, this is a fundamental problem for the definition of Λ's topology and location; though it is always assumed to be real and discrete. On the other hand, this is a practical issue for the numerical computation of T_λ and coefficients c_λ for which no direct orthogonal properties are available from a simple, scalar-product-based, definition.

For a clear understanding of these points, one needs to look back to the origins. Graetz and Nusselt [9, 17] studied a simplified version of the problem: a fluid flowing in a single duct at high Peclet number Pe (which is the ratio of convection to diffusion time scales), when longitudinal diffusion is negligible compared to radial diffusion. The duct is assumed to be either a circular cylinder or made of two parallel infinite plates. Such a symmetric configuration actually leads to simplified one-dimensional problems. In the case of a cylindrical duct, with the radial coordinate denoted by r, one comes back to the Graetz problem

$$\frac{1}{r} \partial_r \left(r \partial_r T \right) = \text{Pe} v(r) \partial_z T,$$

with a Poiseuille parabolic velocity profile $v(r)$. In this simplified framework, searching for a separate variable solution $T(r, z) = f(r)g(z)$, firstly leads after a straightforward calculation to $g(z) = e^{\lambda \text{Pe} z}$ and secondly leads to the eigenvalue problem defining $f(r)$ now denoted $T_\lambda(r) := f(r)$:

$$T(r, z) = T_\lambda(r) e^{\lambda \text{Pe} z}, \qquad \frac{1}{r} \partial_r \left(r \partial_r T_\lambda \right) = \lambda v T_\lambda, \tag{2}$$

which allows the definition of λ/T_λ as eigenvalues/eigenfunctions. Problem (2) is, moreover, symmetric negative, self adjoint with compact resolvent, justifying decomposition (1) where Λ appears as a discrete subset of $\mathbb{R}^-$. Moreover, the coefficients c_λ can be easily computed using scalar products thanks to the symmetry of the system

$$c_\lambda = \int T_0(r) T_\lambda(r) r dr,$$

where T_0 is the inlet condition at $z = 0$.

These results have historically justified (1) as an interesting heuristic. However, as soon as the Graetz-Nusselt framework is perturbed, none of the previous steps

can be performed in a simple way. Indeed, many studies have explored possible extensions to that framework. Among these extensions, two are of particular importance: the extended Graetz problem where the longitudinal diffusion term is no longer neglected, and the conjugated Graetz problem in which coupling with a solid wall where diffusion occurs is considered. We list bellow the difficulties met by previous contributors when considering these extensions.

Looking for a separate variable solution $T(r, z) = f(r)g(z)$ no longer provides in a straightforward way a definition of the type $g(z) = e^{\lambda z}$. However assuming such a usual decomposition $T(r, z) = T_\lambda(r)e^{\lambda z}$, one do not get anymore an eigenvalue problem. Precisely, in the case of the conjugated Graetz problem, the new problem to be solved for T_λ reads:

$$\begin{cases} \frac{1}{r}\partial_r\left(r\partial_r T_\lambda\right) & = \lambda \mathrm{Pe} v T_\lambda \qquad \text{fluid part} \\ \frac{1}{r}\partial_r\left(r\partial_r T_\lambda\right) & = -\lambda^2 T_\lambda \qquad \text{solid part} \end{cases} + \text{coupling condition on the fluid/solid interface,}$$

where the quadratic term λ^2 is accounting for the axial diffusion along z. In such a form, one can see that this problem is not an eigenvalue problem on the whole fluid+solid domain.

Adding axial diffusion now permits information back-flow in the $z < 0$ direction, not only along the flow with $z > 0$. Therefore both positive and negative "*eigenvalues*" λ are physically expected: the previous symmetric-negative structure of the Graetz problem is no longer relevant here. However, until Papoutsakis work [18] detailed below, no attention had been paid to this important point. Early papers on the extended/conjugated Graetz problem [25, 1, 15, 5, 6, 13, 26, 27, 16] assumed a negative "*spectrum*" (that could, at least in principle, be complex) and a complete set of "*eigenfunctions*" by plugging a Graetz-problem-like series solution into the diffusion convection equation.

Still in these early works, as pointed out by Michelsen *et al.* [16], the difficulties of determining both the non-orthogonal "*eigenfunctions*" and the expansion coefficients c_λ appear critical. From a computational point of view the strategy used by Hsu *et al.* [13, 26, 27] using the Gram-Schmidt re-orthogonalization procedure has a high cost, especially when approaching the entrance region where a large number of "*eigenvalues*" is necessary for a correct representation of the solution.

The domain definition and inlet condition also raise new questions and difficulties. In early papers, the flow domain is set as the positive real axis and the assumption of uniform fluid temperature at the inlet has been widely used. As pointed out in [18, 28], e.g., when axial diffusion is permitted, the uniform inlet condition is invalid since the temperature would be altered by upstream conduction before reaching the inlet location.

The most important progress in overcoming these difficulties has been made by Papoutsakis and Ramakrishna in a series of innovative papers [19, 20, 18]. [18] proposes a new formulation of the extended Graetz problem, adding a second unknown temperature flux, leading to a symmetric eigenvalue problem. This approach thus answers the problem regarding the spectrum location (real eigenvalues only) and provides a nice formalism for the amplitude coefficient c_λ computation. This approach has been successfully used in a series of recent papers by Weigand *et al.* [29, 32, 31, 30] and Chi-Dong Ho *et al.* for various heat exchanger configurations,

among which we non-comprehensively quote [11, 12].

In our opinion, three important issues are still pending:

1- Papoutsakis *et al.* formulation only covers symmetrical configurations such as circular ducts or rectangular channels,

2- The extension to the conjugated Graetz problem proposed in [19, 20] (adding solid parts with diffusion) remains heavy and complicated,

3- From a theoretical point of view, only the symmetry of the problem has been proved: neither its self-adjointness nor the resolvent compactness have been proved. In particular the completeness of the eigenvalue set T_λ has not been shown yet, weakening the legitimacy of the proposed decomposition (1).

The aim of this paper is to address these issues in a very general tube configuration (we assume no symmetry of the tube section) for any general unidirectional velocity profile (for example allowing non-Newtonian velocity profiles). A major result we wish to achieve here is to derive a formulation of the initial three-dimensional problem into a two-dimensional one, whose numerical discretization is obviously much easier. The physical and geometrical frameworks are described in section 2. Section 3 develops a theoretical investigation of Equation (1) decomposition for the temperature solution. Subsection 3.1 introduces a reformulation of the problem which allows the search for separate variable solutions and leads to an eigenvalue problem. In subsection 3.2 the functional properties of the eigenvalue problem operator are established. It is proved to be symmetric and moreover self adjoint with a compact resolvent on a basic Hilbert space. At the end of this theoretical section, these results are used in 3.3 to display a full decomposition of a temperature field for which far field conditions are substituted for an inappropriate inlet condition at $z = 0$. This decomposition appears efficient from a computational point of view since it only exhibits the eigenvalues/eigenvectors of the problem as well as easily computable coefficients using simple scalar products. In section 4, it is shown that the eigenvalue problem is naturally equivalent to a mixed variational problem, thus providing a simple computational framework to solve the eigenvalue problem in terms of mixed finite element methods. The remaining part of this section is devoted to the analysis of the numerical convergence of the method. We restrict ourselves to symmetric configurations where analytical solutions are available allowing an *a priori* error estimate of the solution. In this last section we notably study the previously discussed extended Graetz and conjugated Graetz problems.

2   Physical statement

2.1   Geometry, general assumptions and notations

The domain considered here is an infinite cylinder $Z = \Omega \times \mathbb{R}$ having a cross section $\Omega \subset \mathbb{R}^2$ (assumptions on Ω are stated below). The coordinate system relative to Ω will be denoted by (x, y) and the axial coordinate by $z \in \mathbb{R}$.

The domain cross-section Ω is assumed bounded and its boundary $\partial\Omega$ is taken to be smooth (C^1 regularity). Its outward normal is denoted by **n**. Ω is divided into
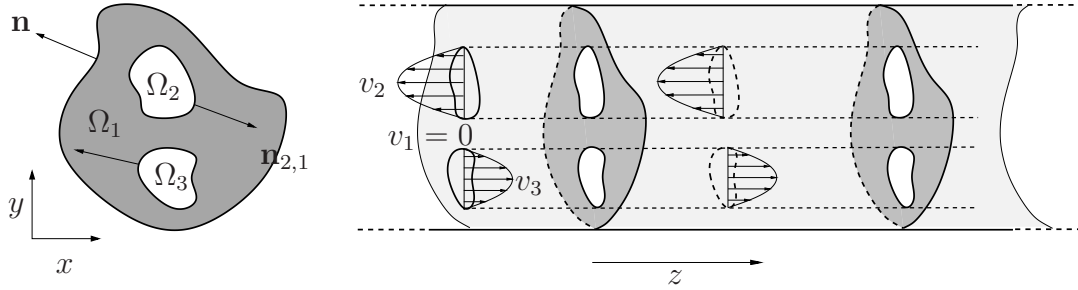
Figure 1: Domain cross-section Ω (left) and whole domain $Z = \Omega \times \mathbb{R}$ (right)

a collection of open sub-domains Ω_i $(1 \leq i \leq N)$ with smooth boundaries, disjoint ($\Omega_i \cap \Omega_j = \emptyset$ if $i \neq j$) and such that $\overline{\Omega} = \cup_i \overline{\Omega_i}$. The interface between Ω_i and Ω_j (if non-empty) is denoted by $\Gamma_{ij} = \overline{\Omega_i} \cap \overline{\Omega_j}$, and its unit normal, outward from Ω_i towards Ω_j, will be denoted by $\mathbf{n}_{ij}$. These assumptions ensure that the semi-norm $\int_\Omega |\nabla u|^2 dx$ is a norm on $H_0^1(\Omega)$ equivalent to the H_1 norm (Poincaré inequality) and also that $H_0^1(\Omega)$ and $H^1(\Omega_i)$ have compact embedding into $L^2(\Omega)$ and $L^2(\Omega_i)$ respectively (see e..g [8, 3]).

The flow in the fluid part is assumed to be established and laminar, so that the velocity $\mathbf{v} = v(x,y)\mathbf{e}_z$ is along the z direction and is a function of (x,y) only. The velocity profile v is only assumed bounded: $v \in L^\infty(\Omega)$, though it is physically continuous in all applications. Solid sub-domains Ω_i are taken into account by setting $v_{|\Omega_i} = 0$. $v > 0$ (*resp.* $v < 0$) on Ω_i naturally means that Ω_i is a fluid sub-domain where the flow is in the $z > 0$ (*resp.* $z < 0$) direction.

The conductivity k is isotropic but heterogeneous. Precisely, k is a bounded, positive and piecewise constant function constant on every Ω_i:

$$0 < \alpha \leq k(x) \leq \beta < +\infty \quad a.e. \ in \ \Omega \ , \quad k_i := k_{|\Omega_i} \in \mathbb{R} \ . \tag{3}$$

$T_i := T_{|\Omega_i}$ indicates the restriction of the function T to the sub-domain Ω_i. Conventionally here, the differential operators div, ∇ are considered on $\mathbb{R}^2$ only: $\mathrm{div}\mathbf{p} = \partial_x p_1 + \partial_y p_2$ and $\nabla f = (\partial_x f, \partial_y f)$, for a vector field $\mathbf{p}$ and a scalar function f respectively.

2.2 Energy equation

On the infinite cylinder $Z = \Omega \times \mathbb{R}$. The dimensionless energy equation is

$$\mathrm{div}(k\nabla T) + k\partial_z^2 T = \mathrm{Pe} \ v \partial_z T \ , \tag{4}$$

where Pe is the dimensionless Péclet number. On the cylinder boundary ∂Z, constant temperatures are imposed, with a step change at the entry $z = 0$:

$$\begin{cases} T_{|\partial Z} = 1 \text{ if } z < 0 \\ T_{|\partial Z} = 0 \text{ if } z > 0 \end{cases} . \tag{5}$$

Relevant limit conditions as $z \to \pm\infty$ therefore are:

$$T(\cdot, z) \underset{z \to -\infty}{\to} 1 \ , \quad T(\cdot, z) \underset{z \to +\infty}{\to} 0 \ . \tag{6}$$

Coupling conditions at the sub-domain interfaces also are required, physically stand-ing for the continuity of the temperature (concentration) and of the normal heat (mass) flux, they read:

$$T_i = T_j \quad \text{and} \quad k_i \nabla T_i \cdot \mathbf{n}_{ij} = k_j \nabla T_j \cdot \mathbf{n}_{ij} \quad \text{on} \quad \Gamma_{ij} \; , \tag{7}$$

whenever the interface Γ_{ij} is non-empty, the dot product naturally standing for the scalar product in $\mathbb{R}^2$.

3   Mathematical analysis

3.1   Problem reformulation

Equation (4) is reformulated into a system of two first order differential equations:

$$\partial_z T = \text{Pe } v \; k^{-1} \; T \;\; - \;\; k^{-1} \text{div}(\mathbf{p}) \tag{8}$$
$$\partial_z \mathbf{p} = k \nabla T \; , \tag{9}$$

where T still denotes the dimensionless temperature (or concentration), the addi-tional unknown $\mathbf{p}$ denotes a vector valued function on Ω.

Introducing the following unbounded operator $A : D(A) \subset \mathcal{H} \mapsto \mathcal{H}$ on an Hilbert space $\mathcal{H}$ and with domain $D(A)$ (whose definitions follow), system (8) takes the form of an ODE on the infinite dimensional space $\mathcal{H}$ with unknown $\Phi(z) \in \mathcal{H}$:

$$\frac{d}{dz}\Phi(z) = A\Phi(z) \; , \quad \Phi(z) = \left| \begin{array}{c} T(z) \\ \mathbf{p}(z) \end{array} \right. \; , \quad A = \left(\begin{array}{cc} \text{Pe } vk^{-1} & -k^{-1}\text{div}(\cdot) \\ k\nabla\cdot & 0 \end{array} \right) \; . \tag{10}$$

The space $\mathcal{H}$ is defined as the Hilbert spaces product $\mathcal{H} = L^2(\Omega) \times (L^2(\Omega))^2$, where $(L^2(\Omega))^2$ is the space of square integrable vector valued functions on Ω. $\mathcal{H}$ is equipped with the following scalar product,

$$(\Psi_1, \Psi_2)_{\mathcal{H}} = \left(\left| \begin{array}{c} T_1 \\ \mathbf{p_1} \end{array} \right. , \left| \begin{array}{c} T_2 \\ \mathbf{p_2} \end{array} \right. \right)_{\mathcal{H}} = \int_{\Omega} T_1 T_2 k dx \;\; + \;\; \int_{\Omega} \mathbf{p_1} \cdot \mathbf{p_2} k^{-1} dx \; . \tag{11}$$

Note that this scalar product on $\mathcal{H}$ is equivalent to the canonical one (taking $k = 1$) by using assumption (3). It has been modified to ensure the symmetry of the operator A.

Relative to a homogeneous Dirichlet boundary condition, the domain $D(A)$ is given as $D(A) := H_0^1(\Omega) \times H(\text{div}, \Omega)$, where $H(\text{div}, \Omega) = \{\mathbf{p} \in (L^2(\Omega))^2, \; \text{div}(\mathbf{p}) \in L^2(\Omega)\}$ in the distribution sense. We shall refer to [4] for the basic properties of the space. Such a definition of $D(A)$ ensures that $A : \; D(A) \subset \mathcal{H} \mapsto \mathcal{H}$ in (10) is well defined.

Proposition 3.1. *The operator A is dense and symmetric:*

$$\forall \; \Psi_1, \Psi_2 \in D(A) \; : \quad (A\Psi_1, \Psi_2)_{\mathcal{H}} = (\Psi_1, A\Psi_2)_{\mathcal{H}} \; . \tag{12}$$

Proof. The density of A directly follows from its definition. Denoting $\Psi_j = \begin{vmatrix} T_j \\ \mathbf{p}_j \end{vmatrix}$,
$j = 1, 2$, using the Green formula and the fact that $T_j \in H_0^1(\Omega)$ yields:

$$
\begin{aligned}
(A\Psi_1, \Psi_2)_{\mathcal{H}} &= \int_{\Omega} \mathrm{Pe}\ v T_1 T_2 dx \ - \ \int_{\Omega} \mathrm{div}\,(\mathbf{p}_1)\, T_2 dx \ + \ \int_{\Omega} \nabla T_1 \cdot \mathbf{p}_2 dx \\
&= \int_{\Omega} \mathrm{Pe}\ v T_2 T_1 dx \ + \ \int_{\Omega} \mathbf{p}_1 \cdot \nabla T_2 dx \ - \ \int_{\Omega} T_1 \mathrm{div}\,(\mathbf{p}_2)\, dx \\
&= (\Psi_1, A\Psi_2)_{\mathcal{H}}\ .
\end{aligned}
$$

$\square$

3.2   Spectral analysis of A

In this section, the main theoretical result of our study is proved. We show that A is self adjoint and that (0 excepted), its spectrum is made of eigenvalues of finite order only, the corresponding eigenfunctions forming a Hilbert (complete) base of $(\mathrm{Ker}\ A)^{\perp} = \mathrm{Ran}\ A$. We observe that denoting by $\Psi_n = (T_n, \mathbf{p}_n)$ the components of the nth eigen-function $(A\Psi_n = \lambda_n \Psi_n)$, and introducing $T(x, y, z) = e^{\lambda_n z} T_n(x, y)$, we have:

$$
\mathrm{div}(k\nabla T_n) + \lambda_n^2 k T_n = \lambda_n \mathrm{Pe}\ v T_n \quad \text{and} \quad \mathrm{div}(k\nabla T) + k\partial_z^2 T = \mathrm{Pe}\ v\partial_z T\ ,
$$

and T is a solution of the original energy equation (4). Incidentally, we also recover the *so-called* eigen-values/functions of the previously quoted literature [1, 2, 6, 5, 13, 26, 27, 15, 25]. This theorem therefore brings full legitimacy to the decompositions routinely found in the literature.

Theorem 3.2. *$A: \ D(A) \subset \mathcal{H} \mapsto \mathcal{H}$ is self-adjoint and has a compact resolvent. We introduce the Kernel of A , $\mathrm{Ker}\ A = \{(0, \mathbf{p}), \ \mathbf{p} \in H_0(div, \Omega)\}$, where $H_0(div, \Omega) = \{\mathbf{p} \in H(div, \Omega), \ div\ \mathbf{p} = 0\}$. Then there exists a Hilbert base $(\Psi_n)_{n \in \mathbb{N}}$ of $Ran\ A = (Ker\ A)^{\perp}$ composed of eigen-functions: $\Psi_n \in D(A)$, $A\Psi_n = \lambda_n \Psi_n$, $\|\Psi_n\|_{\mathcal{H}} = 1$. The coordinates of Ψ_n are denoted $\Psi_n = (T_n, \mathbf{p}_n) = (T_n, k\nabla T_n/\lambda_n)$. We therefore have*

$$
D(A) = \left\{ \Psi \in \mathcal{H}\ , \quad \sum_n |\lambda_n(\Psi, \Psi_n)_{\mathcal{H}}|^2 < +\infty \right\}\ , \quad A\Psi = \sum_n \lambda_n(\Psi, \Psi_n)_{\mathcal{H}}\Psi_n\ ,
$$

for all $\Psi \in D(A)$.
Moreover this base can be split into two parts $\left(\Psi_i^+\right)_{i \in \mathbb{N}}$ and $\left(\Psi_i^-\right)_{i \in \mathbb{N}}$ such that:

$$
0 > \lambda_1^+ \geq \cdots \geq \lambda_j^+ \geq \cdots \to -\infty\ , \quad 0 < \lambda_1^- \leq \cdots \leq \lambda_j^- \leq \cdots \to +\infty\ , \tag{13}
$$

The corresponding eigen-functions are denoted $\Psi_n^{\pm}$. Eigen-values(functions), according to this decomposition, are respectively called upstream (+) and downstream (-) .

In the proof, we shall use the following regularity result (see[14] *p.* 192-196):

Lemma 3.3. *For any $f \in L^2(\Omega)$. there exists a unique $T \in H_0^1(\Omega)$ satisfying $div(k\nabla T) = f$ in the distribution sense. That solution also satisfies on each subdomain Ω_i: $T_i \in H^2(\Omega_i)$, $div(k\nabla T) = f$ in $L^2(\Omega_i)$ (strong sense) and $\|T_i\|_{H^2(\Omega_i)} \leq C\|f\|_{L^2(\Omega)}$ (C independent on f). Moreover T satisfies on every interface $\Gamma_{i,j}$ the coupling conditions (7) in the trace sense.*

Proof. A is dense and symmetric. Since $vk^{-1} \in L^\infty(\Omega)$, A is also a continuous perturbation of the symmetric operator $A_0 : D(A) \subset \mathcal{H} \mapsto \mathcal{H}$ defined as $A_0 = \begin{pmatrix} 0 & -k^{-1}\text{div}(\cdot) \\ k\nabla\cdot & 0 \end{pmatrix}$. Using the Kato-Relish theorem (see e.g. [23] p. 163), the self-adjointness of A_0 implies the self-adjointness of A. To prove the self-adjointness of A_0, one shows that $A_0 + i$ has range $\mathcal{H}$ (see e.g. [22]).

Let us fix $(f, \mathbf{q}) \in \mathcal{H}$. We search for $T \in H_0^1(\Omega)$ such that:

$$\forall \varphi \in H_0^1(\Omega) \;:\; \int_\Omega T\varphi k dx + \int_\Omega k\nabla T \cdot \nabla\varphi dx = \int_\Omega \nabla\varphi \cdot \mathbf{q} dx - \int_\Omega i\varphi f k dx \;.$$

On the right one clearly has a continuous linear form on $H_0^1(\Omega)$, whereas the left side exhibits a symmetric, positive, continuous and coercive bilinear product on $H_0^1(\Omega)$. As a result, the Lax-Milgram theorem applies (see e.g. [8]) ensuring the existence and uniqueness of such a T. Let us define $i\mathbf{p} = \mathbf{q} - k\nabla T \in (L^2(\Omega))^2$. From the above equality we obtain:

$$\forall \varphi \in C_c^\infty(\Omega) \;:\; \int_\Omega i\mathbf{p} \cdot \nabla\varphi dx = \int_\Omega k(if + T)\varphi dx \;.$$

This equality shows that, in the distribution sense, $\text{div}(\mathbf{p}) \in L^2(\Omega)$ and we have $\mathbf{p} \in H(\text{div}, \Omega)$. Thus $\Psi = (T, \mathbf{p}) \in D(A)$ and one has $(A_0 + i)\Psi = (f, \mathbf{q})$, so proving the self adjointness of A_0 and A.

To prove that A has a compact resolvent, we introduce the pseudo inverse of A, $A^{-1} :$ Ran $A \mapsto$ (Ker $A)^\perp \cap D(A) =$ Ran $A \cap D(A)$ and we prove that A^{-1} is compact.

For this let us consider a bounded sequence $(f_n, \mathbf{q}_n) \in$ Ran A. There is a unique $(T_n, \mathbf{p}_n) \in$ Ran $A \cap D(A)$ satisfying $A(T_n, \mathbf{p}_n) = (f_n, \mathbf{q}_n)$. (T_n) then satisfies $k\nabla T_n = \mathbf{q}_n$ and therefore forms a bounded sequence in $H_0^1(\Omega)$. The compact embedding $H_0^1(\Omega) \mapsto L^2(\Omega)$ thus implies that (T_n) is relatively compact in $L^2(\Omega)$.

We now introduce $\varphi_n \in H_0^1(\Omega)$ the unique variational solution to $\text{div}(k\nabla\varphi_n) =$ Pe $vT_n - kf_n$. Let us prove that $\mathbf{p}_n = k\nabla\varphi_n$. Since $A(T_n, k\nabla\varphi_n) = (f_n, \mathbf{q}_n)$, we have to check that $(T_n, k\nabla\varphi_n) \in$ (Ker $A)^\perp$:

$$\forall \mathbf{p} \in H_0(\text{div}, \Omega) : \left(\left. \begin{matrix} T_n \\ k\nabla\varphi_n \end{matrix} \right. , \left. \begin{matrix} 0 \\ \mathbf{p} \end{matrix} \right. \right)_{\mathcal{H}} = \int_\Omega \nabla\varphi_n \cdot \mathbf{p} dx = -\int_\Omega \varphi_n \text{div}(\mathbf{p}) dx = 0$$

Lemma 3.3 then applies and ensures that $\varphi_{n|\Omega_i} \in H^2(\Omega_i)$ and that, (Pe $vT_n - kf_n$), being bounded in $L^2(\Omega)$, $(\varphi_{n|\Omega_i})$ is bounded in $H^2(\Omega_i)$. Therefore both components of $(\nabla\varphi_{n|\Omega_i})$ are bounded in $H^1(\Omega_i)$, thus implying that both components of $(\mathbf{p}_{n|\Omega_i})$

also are bounded in $H^1(\Omega_i)$. The compact embedding $H^1(\Omega_i) \subset L^2(\Omega_i)$ then ensures that $(\mathbf{p}_n)$ is relatively compact in $L^2(\Omega)$.

Consequently, A^{-1} is compact and self adjoint on the separable space Ran A. Therefore there exists a Hilbert base $(\Psi_n)_{n \in \mathbb{N}}$ for Ran A made of eigen-functions: $\Psi_n \in D(A)$, $A\psi_n = \lambda_n \Psi_n$.

A^{-1} being compact, 0 is the only limit point for sub-sequences of $(1/\lambda_n)$ and thus $\{-\infty, +\infty\}$ are the only two possible limit points for sub-sequences of (λ_n). It is easily seen that, whatever the value of $\alpha \in \mathbb{R}$, $A + \alpha$ is bounded neither below nor above. The spectrum is therefore also neither bounded below nor above. Thus $\{-\infty, +\infty\}$ are both limit points for the spectrum, implying decomposition (13).

$\qquad\qquad\qquad\qquad\qquad\qquad\qquad\qquad\qquad\qquad\qquad\qquad\qquad\qquad\qquad\qquad$ $\square$

3.3   Solution derivation

The results of the previous section are used here to derive the solution $\Phi(z) = (T(z), \mathbf{p}(z))$ to (8)-(10) such that T satisfies the boundary, limit and interface conditions in (5)-(6) and (7). We point out that the boundary condition (5) implies that, for $z < 0$, one does not have $\Phi(z) \in D(A)$. For this to be taken into acount, we shall consider the (maximal) extension $\overline{A}$ to operator A:

- $D(\overline{A}) = H^1(\Omega) \times H(\mathrm{div}, \Omega)$,

- $\overline{A} : D(\overline{A}) \mapsto \mathcal{H}$ has the same algebraic expression as A in (10).

Unlike A, $\overline{A}$ is not symmetric:

$$(\overline{A}\Psi_1, \Psi_2)_{\mathcal{H}} = (\Psi_1, \overline{A}\Psi_2)_{\mathcal{H}} + \int_{\partial\Omega} T_1 \mathbf{p}_2 \cdot \mathbf{n} ds - \int_{\partial\Omega} T_2 \mathbf{p}_1 \cdot \mathbf{n} ds \;, \qquad (14)$$

for all pairs of functions in $D(\overline{A})$, with the usual notations.

Definition 3.4. *We shall define a solution to* (8)-(10) *with conditions* (5),(6) *and* (7) *as a function* $\Phi : \; z \in \mathbb{R} \mapsto \Phi(z) = (T(z), \boldsymbol{p}(z)) \in \mathcal{H}$ *such that:*

- $\Phi \in \mathcal{C}\left(\mathbb{R}, \mathcal{H}\right)$ *(continuity on* $\mathbb{R}$*),*

- $\Phi \in \mathcal{C}^1\left(\mathbb{R} - \{0\}, \mathcal{H}\right)$ *(continuous Frechet differentiability on* $\mathbb{R} - \{0\}$*),*

- $\forall z \in \mathbb{R} - \{0\}$, $\Phi(z) \in D(\overline{A})$ *and* $\dfrac{d}{dz}\Phi(z) = \overline{A}\Phi(z)$,

and such that T *satisfies the limit condition* (6) *as* $z \to \pm\infty$ *in* $\mathcal{H}$*'s norm and the boundary, interface conditions* (5)-(7) *for all* $z \neq 0$ *in the trace sense.*

That formalism being stated:

Proposition 3.5. *There exists a unique solution* Φ *to* (8)-(10) *with conditions* (5),(6) *and* (7). *Defining the constants* (α_n),

$$\alpha_n := \frac{1}{\lambda_n^2} \int_{\partial\Omega} k\nabla T_n \cdot \mathbf{n} ds \; = \frac{1}{\lambda_n} \int_{\partial\Omega} \mathbf{p}_n \cdot \mathbf{n} ds, \qquad (15)$$

this solution is given as follows:

$$\Phi(z) = \begin{cases} -\sum_n \alpha_n \Psi_n + \sum_n \alpha_n^- e^{\lambda_n^- z} \Psi_n^- & z \leq 0 \\ -\sum_n \alpha_n^+ e^{\lambda_n^+ z} \Psi_n^+ & z \geq 0 \end{cases} \tag{16}$$

The expression can moreover be simplifyed and the temperature field is given by:

$$T(z) = \begin{cases} 1 + \sum_n \alpha_n^- e^{\lambda_n^- z} T_n^- & z \leq 0 \\ -\sum_n \alpha_n^+ e^{\lambda_n^+ z} T_n^+ & z \geq 0 \end{cases} \tag{17}$$

Since A is not sectoral (is not the infinitesimal generator of an analytic semi-group, see e.g. [10]), some precautions have to be taken in demonstrating the proposition. A detailed proof follows.

Proof. Using the Hilbert base (Ψ_n) of $(\text{Ker } A)^\perp$, the solution Φ is sought in the form $\Phi(z) = \sum_n (\Phi(z), \Psi_n)_{\mathcal{H}} \Psi_n$. All coefficients must therefore satisfy the ODE $\frac{d}{dz}(\Phi(z), \Psi_n)_{\mathcal{H}} = (A\Phi(z), \Psi_n)_{\mathcal{H}}$. Then using (14), the boundary condition (5) and the equality $k\nabla T_n = \lambda_n \mathbf{p}_n$, we find that

$$\frac{d}{dz}(\Phi, \Psi_n)(z) = (\Phi, A\Psi_n)(z) + \omega(z) \int_{\partial\Omega} \mathbf{p}_n \cdot \mathbf{n} ds = \lambda_n (\Phi, \Psi_n)(z) + \lambda_n \alpha_n \omega(z) ,$$

where $\omega(z) = 0$ when $z > 0$ and $\omega(z) = 1$ otherwise. Looking for a bounded and continuous solution to this ODE on $\mathbb{R}$ gives us a unique solution, according to λ_n's sign ($\lambda_n^+ < 0$ and $\lambda_n^- > 0$):

$$(\Phi, \Psi_n^-)(z) = \begin{cases} \alpha_n^- \left(e^{\lambda_n^- z} - 1\right) & z < 0 \\ 0 & z > 0 \end{cases} \quad , \quad (\Phi, \Psi_n^+)(z) = \begin{cases} -\alpha_n^+ & z < 0 \\ -\alpha_n^+ e^{\lambda_n^+ z} & z > 0 \end{cases} .$$

This gives us decomposition (16) and the uniqueness of the solution. Let us now prove that Φ defined by (16) is a solution with the sense in 3.4.
Consider the (unique) function $\varphi_\infty \in H_0^1(\Omega)$ such that $\text{div}(k\nabla\varphi_\infty) = \text{Pe } v$. We introduce $\Phi_\infty = \left| \begin{matrix} 1 \\ k\nabla\varphi_\infty \end{matrix} \right. \in \mathcal{H}$, a function that clearly satisfies $\Phi_\infty \in D(\overline{A})$, $\overline{A}\Phi_\infty = 0$ and $\Phi_\infty \in (\text{Ker } A)^\perp$. Let us prove that $\Phi_\infty = -\sum_n \alpha_n \Psi_n$ (thus explaining how to go from (16) to (17)). Since $\lambda_n \mathbf{p}_n = k\nabla T_n$:

$$(\Phi_\infty, \Psi_n)_{\mathcal{H}} = \int_\Omega T_n k dx + \frac{1}{\lambda_n} \int_\Omega k\nabla\varphi_\infty \cdot k\nabla T_n k^{-1} dx = \int_\Omega T_n k dx - \frac{1}{\lambda_n} \int_\Omega \text{Pe } v T_n dx,$$

and using the equality $\lambda_n k T_n = \text{Pe } v T_n - \frac{1}{\lambda_n} \text{div}(k\nabla T_n)$, we obtain

$$(\Phi_\infty, \Psi_n)_{\mathcal{H}} = -\frac{1}{\lambda_n^2} \int_\Omega k\nabla T_n \cdot \mathbf{n} ds = -\alpha_n .$$

Thus $-\sum_n \alpha_n \Psi_n = \Phi_\infty \in \mathcal{H}$, and it follows that $\Phi_\infty^\pm = -\sum_n \alpha_n^\pm \Psi_n \in \mathcal{H}$ and $\Phi_\infty = \Phi_\infty^- + \Phi_\infty^+$. We use the fact that $\Phi \in D(A)$ if and only if $\sum_n |\lambda_n (\Phi, \Psi_n)_\mathcal{H}|^2 < +\infty$. Since $\lambda_n^+ \underset{n}{\to} -\infty$ (*resp.* $\lambda_n^- \underset{n}{\to} +\infty$), it is straightforward to check that the two functions,

$$f(z) = \sum_n \alpha_n^- \Psi_n^- e^{\lambda_n^- z} \; , \quad g(z) = \sum_n \alpha_n^+ \Psi_n^+ e^{\lambda_n^+ z},$$

satisfy:

- $f \in \mathcal{C}\left((-\infty, 0], \mathcal{H}\right), \; g \in \mathcal{C}\left([0, +\infty), \mathcal{H}\right)$ (continuity),

- $f \in \mathcal{C}^1\left((-\infty, 0), \mathcal{H}\right), \; g \in \mathcal{C}^1\left((0, +\infty), \mathcal{H}\right)$ (continuous Frechet differentiability),

- for $z < 0$ (*resp.* $z > 0$), $f(z) \in D(A)$ (*resp.* $g(z) \in D(A)$) and $\dfrac{d}{dz} f(z) = Af(z)$ (*resp.* $\dfrac{d}{dz} g(z) = Ag(z)$).

The function Φ in (16) can be rewritten as $\Phi(z) = \Phi_\infty + f(z)$, $z \le 0$ and $\Phi(z) = -g(z)$, $z \ge 0$ (which functions actually match at $z = 0$ using $\Phi_\infty = \Phi_\infty^- + \Phi_\infty^+$). It is therefore continuous on $\mathbb{R}$, Frechet differentiable on $\mathbb{R} - \{0\}$, $\Phi(z) \in D(\overline{A})$ and $\dfrac{d}{dz}\Phi(z) = \overline{A}\Phi(z)$ for $z \in \mathbb{R} - \{0\}$ since $\overline{A}\Phi_\infty = 0$. It is also clear that $T(z)$ satisfies the limit condition (6) and the boundary condition (5) for $z \ne 0$.

It remains to be proved that it also satisfies the interface conditions (7) for $z \ne 0$. For this, let us consider the previously introduced function f whose components will be denoted as $f(z) = (t(z), \mathbf{p}(z))$. Since $\lambda_n^- \underset{n}{\to} +\infty$, it is easy to check that, for $z < 0$, $Af(z) \in D(A)$. Therefore $k\nabla t(z) \in H(\mathrm{div}, \Omega)$ which implies that $\mathrm{div}(k\nabla t)(z) \in L^2(\Omega)$ for $z < 0$. Applying 3.3, it follows that $t(z)$ satisfies the interface conditions (7). The same result applies to $g(z)$ for $z > 0$ and, as a result, to $T(z)$ for $z \ne 0$. $\quad\square$

4 Mixed variational formulation and approximation

4.1 Mixed variational formulation

Let us consider the following variational problem: find $(\lambda, T, \mathbf{p}) \in \mathbb{R} \times L^2(\Omega) \times H(\mathrm{div}, \Omega)$ such that, $\forall (u, \mathbf{q}) \in L^2(\Omega) \times H(\mathrm{div}, \Omega)$,

$$\int_\Omega \mathrm{Pe} \; vTudx - \int_\Omega u\,\mathrm{div}(\mathbf{p})dx = \lambda \int_\Omega Tukdx \tag{18}$$

$$-\int_\Omega T\,\mathrm{div}(\mathbf{q})dx = \lambda \int_\Omega \mathbf{p}\cdot\mathbf{q}k^{-1}dx \; . \tag{19}$$

It is clear that whenever Ψ_n is an eigen-function as given in theorem 3.2, then $(\lambda_n, T_n, \mathbf{p}_n)$ satisfies the variational problem above. Conversely if $(\lambda, T, \mathbf{p})$ satisfies (18)-(19) for all $(u, \mathbf{q}) \in L^2(\Omega) \times H(\mathrm{div}, \Omega)$, then the second line implies that $T \in$

$H_0^1(\Omega)$ (using the dense embedding of $H(\text{div}, \Omega)$ into $H^{1/2}(\partial\Omega)'$, see [4]). Therefore $\Psi = (T, \mathbf{p}) \in D(A)$ and satisfies $A\Psi = \lambda\Psi$. Thus $\Psi = \Psi_n$ for some n and solving (18)-(19) is equivalent to finding all the eigen-values/functions of operator A.

4.2 Axi-symmetrical implementation

In order to test this variational formulation, we have derived a one-dimensional version of the problem which is interesting in the case of an axi-symmetrical config-urations. The motivation is to test the convergence of the problem numerically on known solutions. The simplest case is convection-diffusion inside a single cylinder for which, in the limit of large Péclet number, we should recover the Graetz spectrum [9] for the operator A. In this section we consider the somewhat more general case of two concentric cylinders, for which $\Omega = \Omega_1 \cup \Omega_2$, with Ω_1 an inner disk filled with liquid and Ω_2 an outer solid corona. When the size of the second domain to set to zero, the single cylinder problem is found again as a particular case.

A liquid flows inside Ω_1 with a unidirectional, longitudinal, dimensionless velocity $v(r)\mathbf{e}_z$ which varies from a maximal value at the cylinder center $r = 0$ to zero at the boundary with the second cylinder placed at $r = r_0$. We choose the dimensionless velocity to follow the usual Poiseuille flow profile $v(r) = 2\text{Pe}(r_0^2 - r^2)$, although any continuous profile being zero at the boundary could be chosen. The velocity normalization is set so that normalized surface averaged velocity flux is the Péclet number :

$$\frac{1}{\|\Omega_1\|} \int_{\Omega_1} v(r) d\Omega_1 = \text{Pe}$$

Where $\|\Omega_1\| = \pi r_0^2$ is the inner disk area associated with the first inner cylinder section. In corona Ω_2 the velocity is taken to be zero; no convection occurs in this second domain. Continuity of flux and temperature (7) are applied at the domain frontier $\partial\Omega_2 \cap \partial\Omega_2$ with uniform conductivity $k = 1$. The radial dimensionless distance is chosen so that $r = 1$ corresponds to the outer boundary of the second cylinder $\partial\Omega_2 - \partial\Omega_1 \cap \partial\Omega_2$ where a homogeneous Dirichlet boundary condition (5) is chosen.

Problem (18)-(19) is approximated on a regular one-dimensional mesh discretizing coordinate $r \in [0, 1]$ with index i on grid $r = i/n$ with $i \in \{1, n\}$. We adopt here the classical mixed finite element approximation of order 0 of Raviart and Thomas $P_0 \times RT_0$ (see e.g. [4]) to the present axi-symmetrical 1D formulation. Base elements for the scalar T are therefore P_0 piecewise constant functions over the grid elements, whereas base elements for the 'vector' $\mathbf{p}$ are the P_1 continuous piecewise affine functions over the grid elements: thus re-establishing the flux continuity at the grid points.

The generalized linear eigenvalue problem resulting from this discretization choice is as follows:

$$A\Psi_n = \begin{pmatrix} \mathbf{a} & \mathbf{b} \\ \mathbf{b^T} & 0 \end{pmatrix} \Psi_n = \lambda_n \begin{pmatrix} \mathbf{c} & 0 \\ 0 & \mathbf{d} \end{pmatrix} \Psi_n, \tag{20}$$

Where Ψ_n is a $2n$ component vector whose first n components are the discrete temperature field $T_n = (T_i)_{i \in \{1,n\}}$ approximating T_λ and the following $n + 1$ to $2n$

components describe p_n approximating the gradient field $\mathbf{p}_\lambda = \partial_r T_\lambda / \lambda$ which is one-dimensional in this axi-symetrical context. The $n \times n$ matrices $\mathbf{a}$, $\mathbf{b}$, $\mathbf{c}$ and $\mathbf{d}$ can be computed analytically and admit the following coefficients :

$$
\begin{array}{rcc}
a_{ij} & = & -\delta_{ij} \frac{\mathrm{Pe}}{2 r_0 n^4}(2i-1)(2i^2 - 2i - 2r_0^2 n^2 + 1) \\
b_{ij} & = & -\frac{1}{n} (\delta_{ij} i + \delta_{i-1 j}(1-i)) \\
c_{ij} & = & \delta_{ij} \frac{2i-1}{2n^2} \\
d_{ij} & = & -\frac{1}{12 n^2} (\delta_{ij} 8i + \delta_{i-1 j}(2i-1) + \delta_{i+1 j}(2i+1)) ,
\end{array}
\tag{21}
$$

where $(i,j) \in \{1,n\}^2$ and δ is the Kronecker symbol.

4.3   Numerical results and convergence

In the generalized eigenvalue problem (20), one notes that the matrice A is symmetric and that the right hand side mass-matrix $\mathrm{Diag}(\mathbf{c}, \mathbf{d})$ is symmetric positive definite. Therefore, problem (20) can be numerically solved using the variant of the Lanczos algorithm for generalized eigenvalue problems (see e.g. [24]). The resulting first eigenvectors and eigenvalues were computed using the Fortran library ARPACK and sparce matrix storage. The results presented here correspond to two particular configurations:

- a single cylinder with a single radial domain Ω_1 for which $r_0 = 1$ and,

- two concentric cylinders whose radius ratio is two, so that $r_0 = 1/2$.

We study the numerical convergence of the first eigenvalues and first eigenvectors when the Péclet number is varied from low to high values. We systematically compared the discrete numerical results with reference solutions obtained with another iterative method explained in the appendix A.

4.3.1   Single cylinder : $r_0 = 1$

In the case of a single cylinder, for large values of the Péclet number, the upstream part of A's spectrum (positive eigenvalues λ_n^- associated with the $z < 0$ region) is difficult to compute numerically for it diverges with Pe [21]. In contrast, the downstream part of the spectrum (negative eigenvalues λ_n^+ associated with the $z > 0$ region) converges to the Graetz spectrum, and decays to zero as $1/\mathrm{Pe}$ when the Péclet number increases.

Let us first discuss the eigenvalue convergence. Figure 2 illustrates the relative error $E = \sqrt{(\lambda_n - \lambda)^2}/\lambda$ associated with the first two downstream eigenvalues λ_1^+ and λ_2^+ and for the first upstream one λ_1^-. it can be seen in this figure that the convergence of the numerical estimation is consistent with the chosen classical mixed finite element approximation space $P_0 \times RT_0$, for which a $\sim 1/n$ behavior is expected. Furthermore, the strong influence of the Péclet number on convergence rate can also be observed. For small Péclet number, the spectrum is almost symmetrical, so that one expects the convergence for λ_1^+ and λ_1^- to be very close, as observed on figure 2a. In contrast, as the Péclet number increases, there is a distinct shift in the convergence curve. The closer the eigenvalue is to zero, the easier it is to compute.
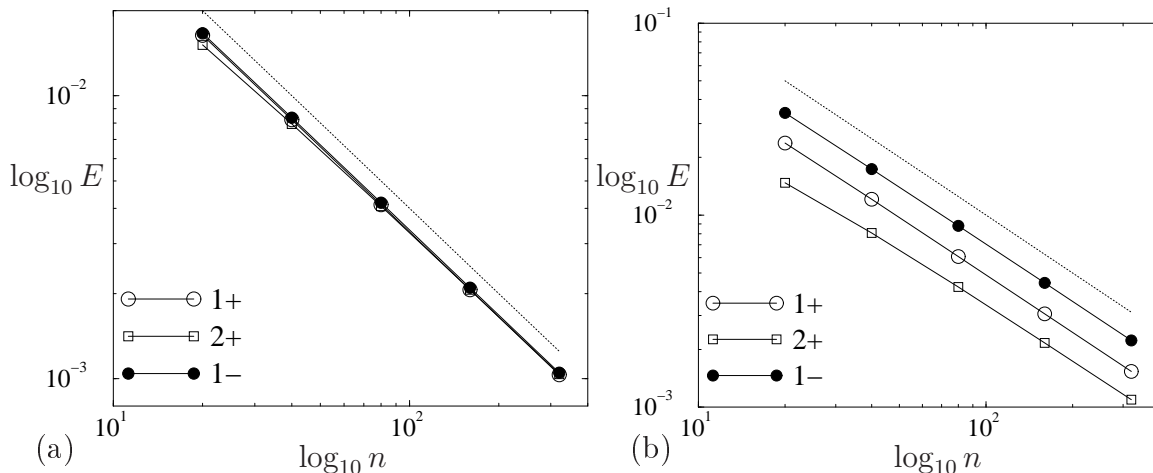
Figure 2: (a) Relative numerical error for eigenvalue λ_1^+, λ_2^+ and λ_1^- for $Pe = 0.1$. The dotted lines corresponds to a -1 slope associated with a $\sim 1/n$ behavior. (b) Same convention as (a) for $Pe = 10$.

Since λ_1^- diverges with Pe, it is more difficult to approximate numerically and, then, the relative error associated with λ_1^- in figure 2b is 30% larger than the one associated with λ_1^+ for $Pe = 10$. This difference further increases with Péclet number. We also wish to illustrate the numerical convergence on the eigenfunction. Figure 3 illustrates the eigenvector computation for the temperature and gradient fields associated with λ_1^+, λ_2^+ and λ_1^- eigenvalues. In the case of small Péclet numbers, the asymptotic symmetry of the eigenvalue spectrum also implies a symmetry of the eigenvectors,dswhich is clearly visible when comparing the $1+$ and $1-$ fields in Figure 3. The associated leading order eigenfunction shows a single maximum at $r = 0$, the cylinder center, and obviously decreases to zero at $r = 1$ for the Dirichlet boundary condition to be fulfilled. When the associated eigenvalue order increases, the corresponding eigenfunction has as many oscillations as the eigenvalue order. For example for λ_2^+, two critical points can be seen, a minimum and a maximum, for the eigenfunction in Figure 3. The superposition between the discrete numerical computation and the "exact" solution is also illustrated in Figure 3. One can see that the comparison for the gradient depicted in Figure 3(b) is rough for $n = 20$, but no difference is visible between the two for $n = 320$ in Figure 3(d). The convergence to the exact solution is also illustrated in figure 4 for $Pe = 10$. In this case the two eigenfunctions associated with λ_1^+ and λ_1^- differ markedly. The first one, associated with λ_1^+, still reaches a maximum at the tube center $r = 0$, whereas the maximum position of the second one, associated with λ_1^-, is shifted close to the tube boundary at $r = 1$. Furthermore, this second eigenfunction decays to zero at the tube center. The reason for this distinct behavior is now the opposite role of convection for these two temperature profiles. For the downstream eigenfunction associated with λ_1^+, longitudinal convection prevails over diffusion. Since this convection is maximum at the tube center, it dictates the shape of the corresponding temperature profile. For the upstream eigenfunction associated with λ_1^-, retro-diffusion is the only mechanism for this temperature to display a back-flow exponential decay. Hence, since the convection is maximal at the tube center, retro-diffusion is maximum at the tube
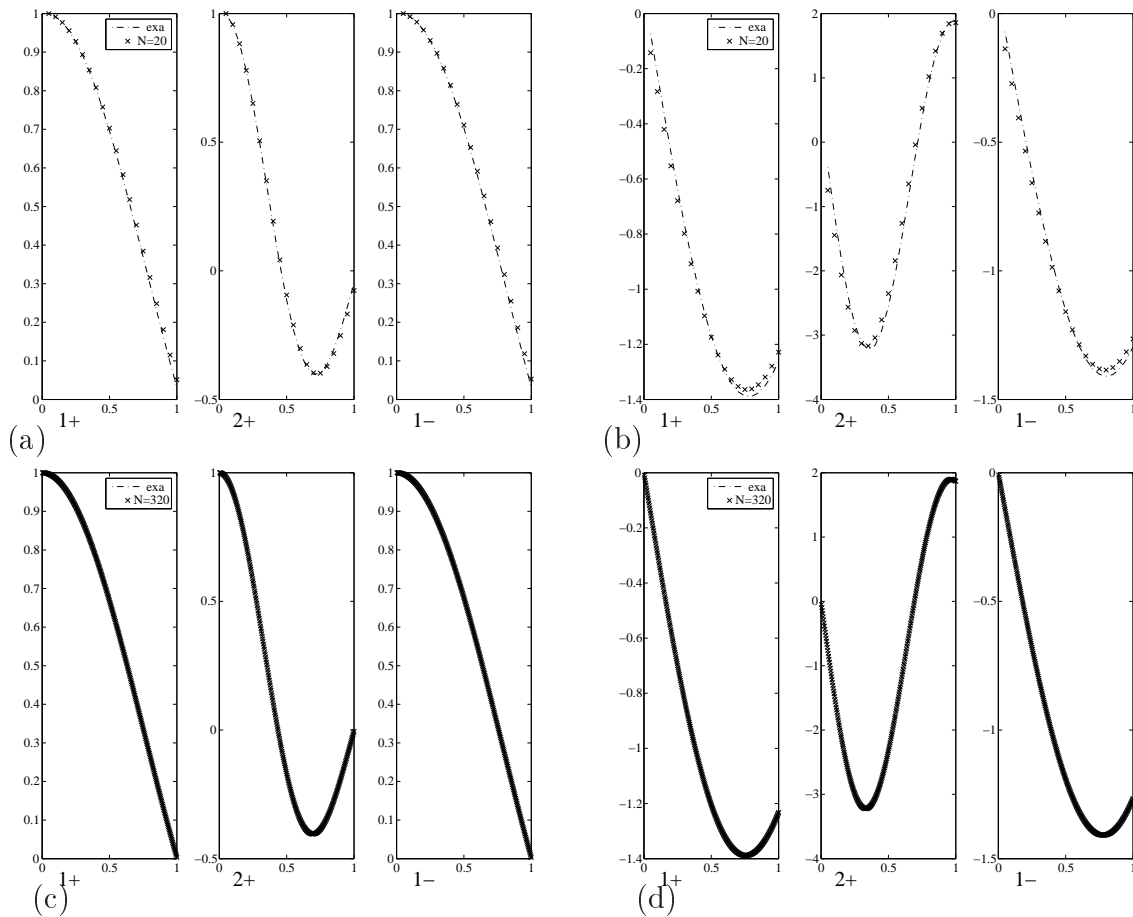
Figure 3: (a) Temperature field $T(i/n)\, i \in \{1, n\}$ for discretization $n = 20$ and Pe $= 0.1$ for the first two downstream eigenvectors 1+ and 2+ and the first upstream eigenvector 1−. Normalization $T(0) = 1$ has been imposed. (b) Temperature gradient $p = \partial_r T(i/n)/\lambda$ for discretization $n = 20$ and Pe $= 0.1$. (c) Same convention as (a) for discretization $n = 320$. (d) Same convention as (b) for discretization $n = 320$.

boundary, where the velocity vanishes. A boundary layer develops near $r = 1$, the thickness of which decays to zero as the Péclet number diverges. This boundary layer is responsible for the numerical difficulties arising in the computation of the upstream part of the spectrum at large Péclet numbers. The slower convergence of the eigenvectors 1− is clearly visible in figure 4a and 4b for a rough discretization of $n = 20$ points. Although in this case, the first two downstream eigenfunctions, 1+ and 2+ are well approximated by the corresponding eigenvectors, this is not the case for the upstream one 1−. Nevertheless, for a sufficient discretization of $n = 320$ points, the convergence can be satisfactory as illustrated on figure 4c,d.

We finally wish to illustrate the convergence on the eigenvector by computing the relative error $E = \sqrt{(\Psi_n - \Psi, \Psi_n - \Psi)_{\mathcal{H}}/(\Psi, \Psi)_{\mathcal{H}}}$ built with the $\mathcal{H}$ norm (11) for a discrete eigenvector Ψ_n to converge to the theoretical one Ψ. Figure 5 shows the convergence of the relative error for increasing point number n. As expected, $1/n$ behavior is observed for both $Pe = 0.1$ and $Pe = 10$, but the error is larger in the latter case.
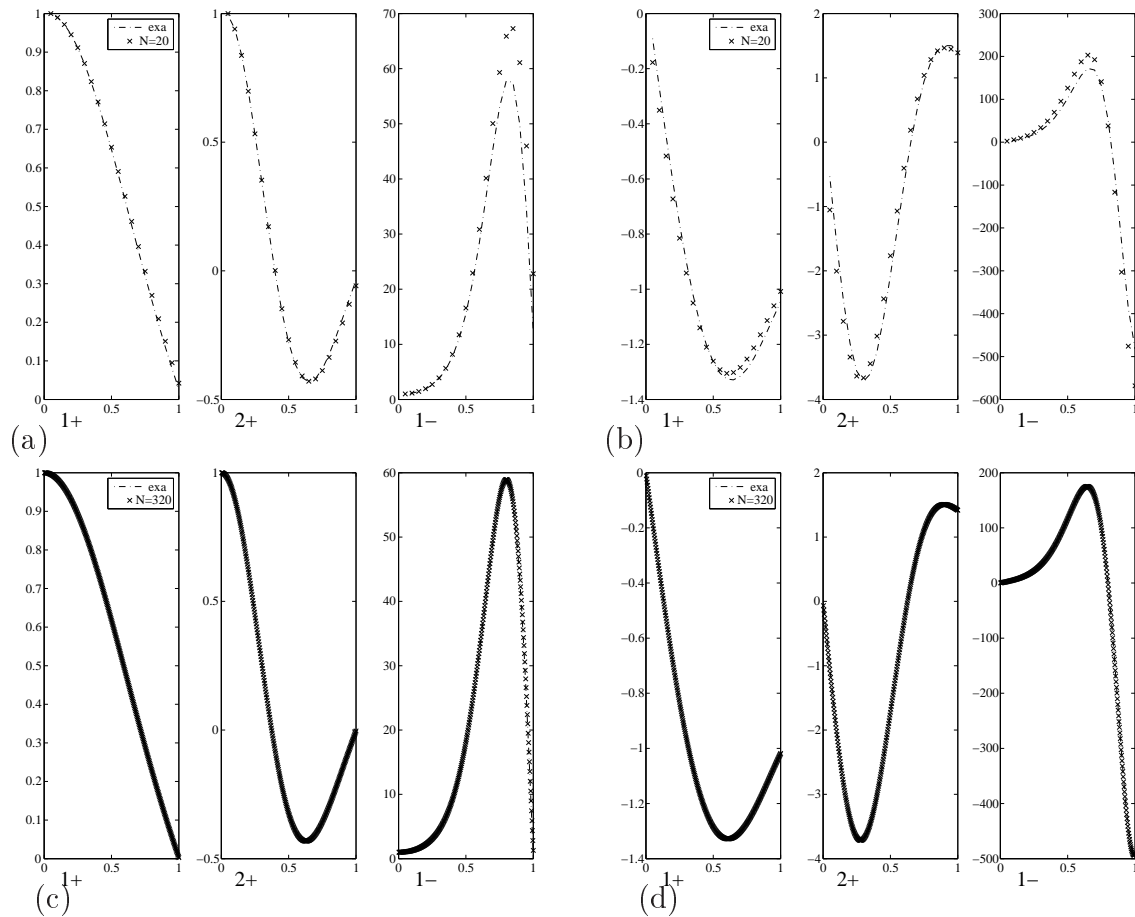
Figure 4: Same conventions as figure 3 for Pe = 10.
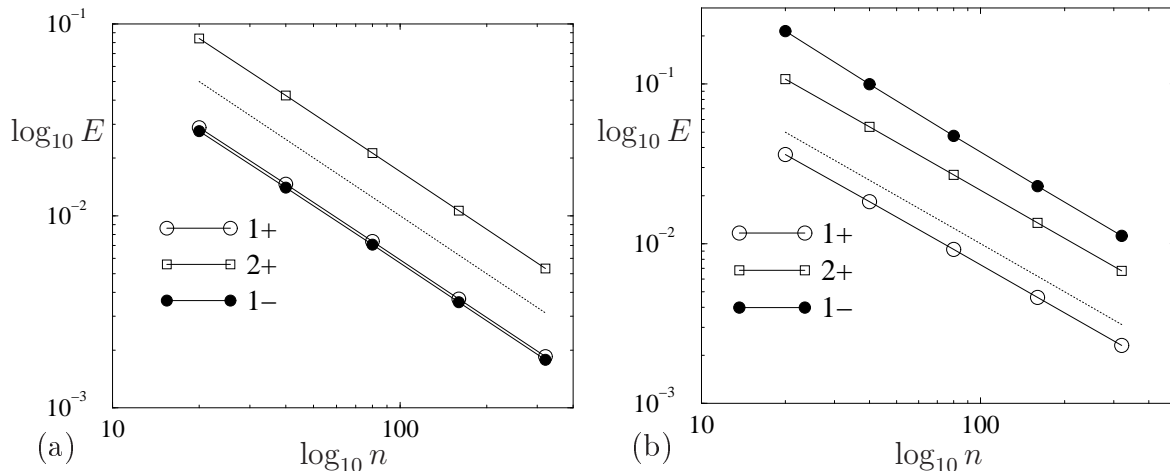
Figure 5: (a) Relative error for eigenvectors associated with eigenvalues λ_1^+, λ_2^+ and λ_1^- for $Pe = 0.1$. The dotted lines corresponds to a -1 slope associated with a $\sim 1/n$ behavior. (b) Same convention as (a) for $Pe = 10$.

4.3.2 Two concentric cylinders : $r_0 = 1/2$

In the case where two domains are present, it is interesting to test the numerical implementation of the flux and temperature continuity (7) between the two domains in this formulation. Figure 6 shows some eigenfunction profiles at the same Péclet

numbers as those previously illustrated for the single cylinder case, Pe = 0.1 and Pe = 10. It can be observed on this figure that the temperature continuity at the

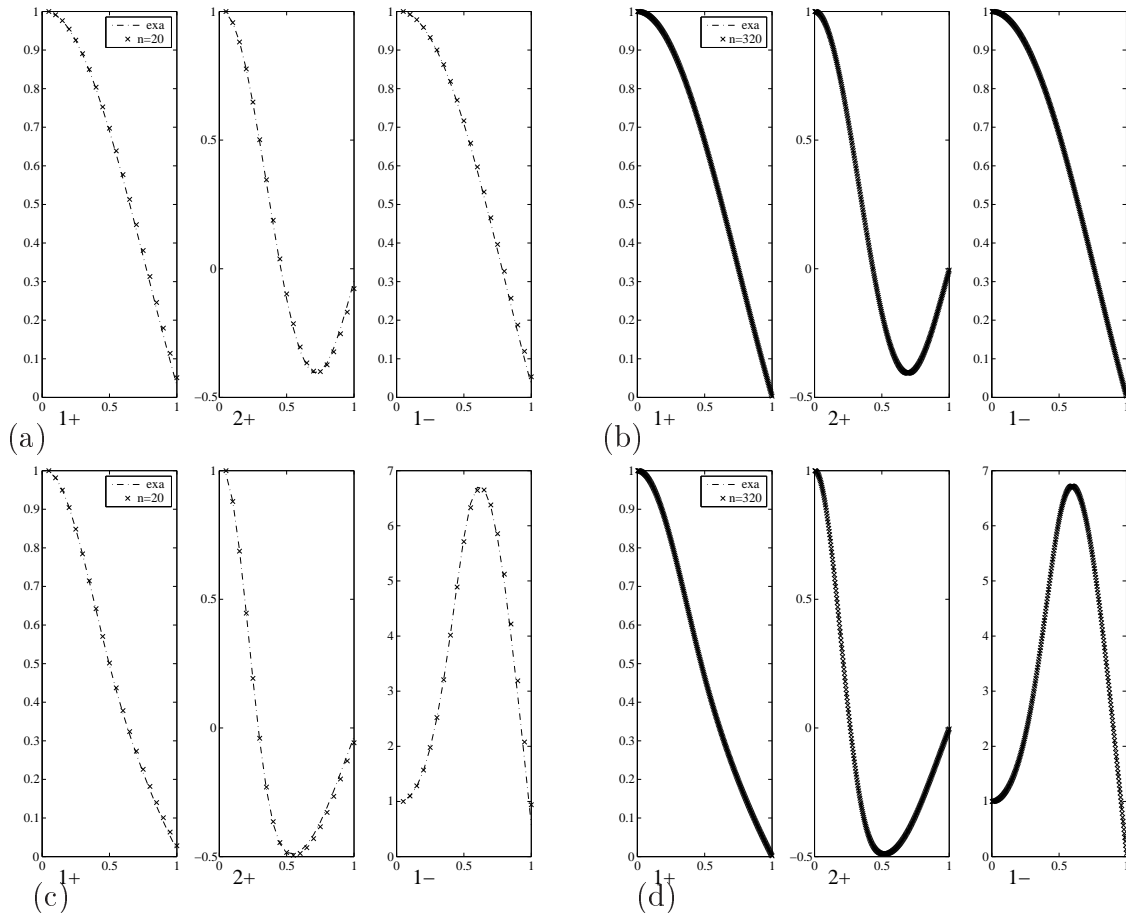Figure 6: (a) Temperature field $T(i/n)\, i \in \{1, n\}$ for discretization $n = 20$ and Pe = 0.1 for the first two positive eigenvectors 1+ and 2+ and the first negative eigenvector 1−. Normalization $T(0) = 1$ has been imposed. (b) Same convection as (a) for for discretization $n = 320$. (c) Same convention as (a) $Pe = 10$. (d) Same convention as (b) for discretization $n = 320$.

domain border $r = r_0 = 1/2$ is excellent even for a modest discretization $n = 20$. The same observation can be made on the gradient field. The convergence to the exact solution which can be visually checked on figure 6c is better than the one previously obtained with the same parameter in figure 4a. This is due to the fact that there is no boundary layer in the latter case when two domains are present. The retro-diffusion of the upstream eigenvector 1− is possible in the second annular domain Ω_2, so that it is not confined in a small region near the boundary. The resulting temperature gradients are much lower and do not diverge with the Péclet number. Hence, the maximum temperature observed for the 1− eigenvector of figures 6c and 6d is indeed localized inside the second domain at a radial coordinate larger than 1/2. Obviously, the temperature values associated with this maximum are much lower than in the case of the single cylinder, due to the smoothing effect associated with permitting retro-diffusion in the second domain Ω_2.

The convergence rate, which can be computed either for the eigenvalues or the eigenvectors, follows the same scaling as those already found for the single cylinder

case. The convergence rate is only a little better (not shown).

5 Conclusion

This paper has presented a new approach for complex three-dimensional configurations of convection-diffusion in unidirectional flows. We justify a separate variable solution approach by defining the eigenvalue/eigenfunction decomposition of an appropriate mixed operator. The theoretical analysis shows that the properties of this operator allow a non-sectorial decomposition of the solution in longitudinally exponentially decaying solutions. This approach permits full three-dimensional problem to be numerically restricted to two-dimensions. Furthermore, a naturally efficient numerical discretization has been proposed using finite-elements. The relevance and efficiency of such a discretization has been analyzed in simple configurations.

References

[1] Aleksashenko, V.A.: Conjugate stationary problem of heat transfer with a moving fluid in a semi-infinite tube allowing for viscous dissipation. J. Eng. Physics and Thermophysics **14**(1), 55–58 (1968)

[2] Belyaev, N.M., Kordyuk, O.L., Ryadno, A.A.: Conjugate problem of steady heat exchange in the laminar flow of an incompressible fluid in a flat channel. J. Eng. Physics and Thermophysics **30**(3), 339–344 (1976)

[3] Brezis, H.: Analyse fonctionnelle, Théorie and applications. Masson (1983)

[4] Brezzi, F., Fortin, M.: Mixed and hybrid finite element methods. Springer Series in Computational Mathematics. (1991)

[5] Davis, E.J., Gill, W.: The effects of axial conduction in the wall on heat transfer with laminar flow. Int. J. Heat Mass Transfer **13**, 459–470 (1970)

[6] Davis, E.J., Venkatesh, S.: The solution of conjugated multiphase heat and mass transfer problems. Chem. Eng. Sci **34**, 775–787 (1978)

[7] Deen, W.: Analysis of transport phenomena. Oxford University press (1998)

[8] Gilbarg, D., Trudinger, N.: Elliptic partial differential equations of second order, *Grundlehren der Mathematischen Wissenschaften*, vol. 224, second edn. Springer-Verlag, Berlin (1983)

[9] Graetz, L.: Uber die Wärmeleitungsfähigkeit von Flüssigkeiten. Annalen der Physik **261**,(7), 337–357 (1885)

[10] Henry, D.: Geometric theory of semilinear parabolic equations. Springer-Verlag, LNM 840 (1981)

[11] Ho, C., Yeh, H., Yang, W.: Double-pass Flow Heat Transfer In A Circular Conduit By Inserting A Concentric Tube For Improved Performance. Chem. Eng. Comm. **192**(2), 237–255 (2005)

[12] Ho, C.D., Yeh, H.M., Yang, W.Y.: Improvement in performance on laminar counterflow concentric circular heat exchangers with external refluxes. Int. J. Heat and Mass Transfer **45**(17), 3559–3569 (2002)

[13] Hsu, C.J.: Theoretical Solutions for low-Peclet-number thermal entry Region that Transfer in laminar Flow through concentric Annuli. Int. J. Heat Mass Transfer **13**, 1907–24 (1970)

[14] Ladyzenskaja, O.A., Ural'ceva, N.N.: Equations aux dérivées partielles de type elliptique. Monographies Universitaires de Mathématiques, No. 31. Dunod, Paris (1968)

[15] Luikov, A., Aleksashenko, V., Aleksashenko, A.: Analytical methods of solution of conjugated problems in convective heat transfer. Int. J. Heat Mass Transfer **14**, 1047–1056 (1971)

[16] Michelsen, M., Villadsen, J.: The Graetz problem with axial heat conduction. Int. J. Heat Mass Transfer **17**, 1391–1402 (1973)

[17] Nusselt, W.: Die abhängigkeit der wärmeübergangszahl von der rohrlänge. Z. Ver. Deut. Ing. **54**, 1154 1158 (1910)

[18] Papoutsakis, E., Ramkrishna, D., Lim, H.C.: The extended Graetz problem with Dirichlet wall boundary conditions. Appl. Sci. Res. **36**, 13–34 (1980)

[19] Papoutsakis, E., Ramkrishna, D., Lim, H.C.: Conjugated Graetz problems. Pt.1: general formalism and a class of solid-fluid problems. Chemical Engineering Science **36**(8), 1381–1391 (1981)

[20] Papoutsakis, E., Ramkrishna, D., Lim, H.C.: Conjugated Graetz problems. Pt.2: fluid-fluid problems. Chemical Engineering Science **36**(8), 1392–1399 (1981)

[21] Pierre, C., Plouraboue, F.: Stationary convection diffusion between two co-axial cylinders. Int J. Heat Mass Transfer **50**(23-24), 4901–4907 (2007)

[22] Reed, M., Simon, B.: Methods of modern mathematical physics. I. Functional Analysis. Academic Press, New York (1975)

[23] Reed, M., Simon, B.: Methods of modern mathematical physics. II. Fourier analysis, self-adjointness. Academic Press, New York (1975)

[24] Saad, Y.: Numerical methods for large eigenvalue problems. Manchester University press. (1991)

[25] Shapovalov, V.V.: Heat transfer in laminar flow of an incompressible fluid in a round tube. J. Eng. Physics and Thermophysics **12**(5) (1967)

[26] Tan, C.W., Hsu, C.J.: Mass Transfer of Decaying Products with Axial Diffusion in Cylindrical Tubes. Int. J. Heat Mass Transfer **13**, 1887–1905 (1970)

[27] Tan, C.W., Hsu, C.J.: Low Peclet number mass transfer in laminar flow through circular 7. tubes. Int. J. Heat Mass Transfer **15**, 2187–2201 (1972)

[28] Telles, A., Queiroz, E., Filho, G.: Solutions of the extended Graetz problem. Int. J. Heat Mass Transfer **44**(2), 471–483 (2001)

[29] Weigand, B.: An extract analytical solution for the extended turbulent Graetz problem with Dirichlet wall boundary conditions for pipe and channel flows. Int. J. Heat Mass Transfer **39**(8), 1625–1637 (1996)

[30] Weigand, B., Gassner, G.: The effect of wall conduction for the extended Graetz problem for laminar and turbulent channel flows. Int. J. Heat Mass Transfer **50**(5-6), 1097–1105 (2007)

[31] Weigand, B., Kanzamar, M., Beer, H.: The extended Graetz problem with piecewise constant wall heat flux for pipe and channel flows. Int. J. Heat Mass Transfer **44**(20), 3941–3952 (2001)

[32] Weigand, B., Wrona, F.: The extended Graetz problem with piecewise constant wall heat flux for laminar and turbulent flows inside concentric. Heat and Mass Transfer **39**(4), 1432–1181 (2003)

A   Reference solutions in axi-symmetrical problems

In this appendix, we give some details about the analytical method used in 4 for the analysis of the numerical results. The method is based on a property of the eigenfunctions called $\lambda-analycity$: in the axi-symmetrical framework, any eigenfunction T_λ can be the expanded in the form

$$T_\lambda(r) \;=\; \sum_{n \in \mathbb{N}} t_n(r)\ \lambda^n \;. \tag{22}$$

In this description the *closure functions* $\{t_n\}_{n \in \mathbb{N}}$ are independent of the eigenvalue λ considered and also of the considered boundary condition at $r = 1$. They can be computed using a simple iterative process for the computation of the spectrum and eigenfunctions with a *Maple* code.

The convergence of the λ-analycity method has been established for general axi-symmetrical configurations. The proof being the topic of a forecoming paper, and for the sake of simplicity, we focus our attention here on the treatment of the Graetz problem. In this case, the proof for the convergence of the λ-analycity method is available in [21]. The eigenvalues T_λ are defined as follows, on the interval $[0, 1]$:

$$T_\lambda(0) = 1 \;, \quad \Delta_c T_\lambda = v(r)\lambda T \;,$$

where Δ_c stands for the cylindrical part of the Laplace operator $\Delta_c \equiv 1/r\partial_r(r\partial_r)$. Eigenfunctions T_λ then read (22) where the $t_n(r)$ fulfill the recursive scheme:

$$t_0(r) = 1 \quad \text{and:} \quad \Delta_c t_n = v(r)t_{n-1}(r) , \quad t_n(0) = 0 \quad \text{for} \quad n \geq 1 .$$

We point out that this scheme actually has a unique solution thanks to the degeneracy of the ODE at $r = 0$.

The spectrum, in the case of a Dirichlet boundary condition, is thus defined as:

$$\Lambda = \left\{ \lambda , \quad \sum_{n\in\mathbb{N}} t_n(1) \, \lambda^n = 0 \right\} .$$

It can be approximated using truncations, with an exponential rate of convergence.